

# Investigation and Development of the Methodologies for Simulating Self-similar Processes

Qidi Peng\* and William Wu<sup>†</sup>

## Abstract

This paper is devoted to the study of simulating a large class of self-similar processes. Since most current simulation approaches are limited to case-by-case studies, every existing approach has its constraints and flaws; hence a general and efficient simulation approach is in demand. Our study sheds some light in this direction. The paper's contributions are bi-fold. First, reviews and improvements are made to some existing methods for simulating specific self-similar processes. Second, we propose a novel method to simulate a general self-similar process, where we use a modified inverse Lamperti transformation to transform self-similarity to stationarity. Successful applications are made to simulate fractional Brownian motion and sub-fractional Brownian motion.

**Keywords:** Simulation; self-similar process; fractional process; stationary process; Lamperti transformation

**MSC (2010):** 60G18, 60G22, 60G10, 65C10

## 1 Introduction

Self-similar processes are an essential and large class of stochastic processes that exhibit the phenomenon of “self-similarity”. That means part of the process's path behaves similarly to its entire path. Self-similarity is featured in many classical stochastic processes in probability theory, such as Brownian motion, fractional Brownian motion [36], linear fractional stable motion [44], fractional Poisson process [31], and Rosenblatt process [17, 48]. Some random fields and random sheets also exhibit self-similarity, with examples such as fractional Brownian fields [16], linear fractional stable fields and sheets [4, 15], etc. It should be noted that self-similar processes can be naturally extended to locally asymptotically self-similar processes [11], with multifractional Brownian motion and linear multifractional stable motion being pragmatic examples [33, 7, 45, 15]. Modern applications of self-similar processes include modeling instrument values in finance, volume of flows in hydrology, weather conditions in meteorology, atomic movement in material science and physics, etc. [43, 22, 19, 47]. In the literature, “simulation of self-similar process” has received wide attention. For example, simulations of fractional ARIMA [45], fractional Brownian motion [20], linear fractional stable motion [45], and self-similar teletraffic [26] have been heavily studied. So far, the methods for simulating self-similar processes work case by case and each has its flaws and constraints. Indeed, [20] in Chapter 7 stated that “very little specific tools are available” for simulating a general self-similar process.

---

\*Corresponding author. Institute of Mathematical Sciences, Claremont Graduate University. Email: qidi.peng@cgu.edu.

<sup>†</sup>Rancho Cucamonga High School. Email: www49387@gmail.com

In the following sections, we list some main existing simulation methodologies for self-similar processes. We explain how the above methods are applied to simulate particular self-similar processes and discuss their pros and cons. Furthermore, we develop a new method to overcome the issues displayed by the above approaches. Therefore, the goals of this paper are the following:

- (i) We investigate and summarize simulation methodologies existing in the literature for a number of well-known self-similar processes. We provide pseudocodes and sources of implementations of these simulation algorithms, and discuss their pros and cons.
- (ii) We develop a novel method for simulating self-similar Gaussian process based on a modified inverse Lamperti transformation. This method has the potential to be extended for simulating more general self-similar processes.

Through this paper, we classify self-similar processes into stationary increments Gaussian processes, processes with integral representations, and processes with wavelet decompositions.

The paper is organized as follows. In Sections 2 - 5, we investigate, respectively, the existing simulation approaches for stationary increments self-similar processes, multifractional Brownian motion, self-similar processes with non-stationary increments, and linear fractional stable motion. These examples cover self-similar processes from Gaussian processes to non-Gaussian ones and from stationary increments processes to non-stationary increments ones. Moreover, we discuss simulation of locally asymptotically self-similar processes, which are natural extensions of self-similar processes. Our significant contribution is in Section 6, where a brand new simulation algorithm is introduced to simulate Gaussian self-similar processes. This method is based on a modified inverse Lamperti transformation and it has the potential to be applied to simulate a large family of self-similar processes. We take the simulation of fractional Brownian motion and sub-fractional Brownian motion as two examples. In Section 7, we conclude.

## 2 Simulation of Stationary Increments Self-similar Gaussian Processes

The self-similar process considered in this paper is defined below.

**Definition 2.1** *We say  $X = \{X(t)\}_{t \in \mathbb{R}}$  is a self-similar process with self-similarity index  $H \in (0, 1)$ , if*

$$\{X(at)\}_{t \in \mathbb{R}} \stackrel{\text{f.d.d.}}{=} \{|a|^H X(t)\}_{t \in \mathbb{R}}, \text{ for any } a \neq 0, \quad (2.1)$$

where  $\stackrel{\text{f.d.d.}}{=}$  denotes equality in finite dimensional distribution: for two stochastic processes  $\{X(t)\}_{t \in \mathbb{R}}$  and  $\{Y(t)\}_{t \in \mathbb{R}}$ ,  $\{X(t)\}_{t \in \mathbb{R}} \stackrel{\text{f.d.d.}}{=} \{Y(t)\}_{t \in \mathbb{R}}$  means  $(X(t_i))_{i=1, \dots, n} \stackrel{\text{law}}{=} (Y(t_i))_{i=1, \dots, n}$  for any  $n \geq 1$  and any  $t_1, \dots, t_n \in \mathbb{R}$ .

Let  $\{X(t)\}_{t \geq 0}$  be a self-similar process. By self-similarity, it suffices to simulate the sample path of  $\{X(t)\}_{t \in [0, 1]}$  in order to obtain any sample paths of  $\{X(t)\}_{t \in [a, b]}$  for  $0 < a < b$ , because (see (2.1))

$$\{X(t)\}_{t \in [a, b]} \stackrel{\text{f.d.d.}}{=} \{b^H X(t)\}_{t \in [a/b, 1]}.$$

Therefore, in the rest of the paper, we only consider simulating a discretized path of  $\{X(t)\}_{t \in [0, 1]}$ :  $(X(1/N), X(2/N), \dots, X((N-1)/N), X(1))$ , where  $N$  denotes the number of nodes in the trajectory. The major techniques in play are Cholesky's decomposition and fast Fourier transformation.

The simulation approaches introduced in this section apply to Brownian motion, fractional Brownian motion, fractional Gaussian noise, fractional ARIMA, and fractional teletraffic data process.

Recall that a fractional Brownian motion  $\{B^H(t)\}_{t \in \mathbb{R}}$  with Hurst parameter  $H \in (0, 1)$  [28, 36] is a zero-mean Gaussian stochastic process with almost surely  $B^H(0) = 0$ , continuous trajectories, and its covariance function is given by: for  $s, t \in \mathbb{R}$ ,

$$\mathbb{C}ov(B^H(s), B^H(t)) = \frac{1}{2} (|t|^{2H} + |s|^{2H} - |t - s|^{2H}). \quad (2.2)$$

Note that when  $H = 1/2$ , the fractional Brownian motion becomes a standard Brownian motion, denoted by  $\{B(t)\}_{t \in \mathbb{R}}$ . Since  $\{B(t)\}_{t \in [0,1]}$  is a Lévy process (it has independent stationary increments), it can be decomposed into the cumulative sum of Gaussian white noise:

$$\begin{cases} B(0) = 0 \text{ a.s.}; \\ B\left(\frac{k}{N}\right) = \sum_{j=0}^{k-1} \varepsilon_{j,N}, \quad \text{for } k = 1, \dots, N, \end{cases} \quad (2.3)$$

where  $\{\varepsilon_{j,N}\}_{j \in \{0, \dots, N-1\}} = \{B((j+1)/N) - B(j/N)\}_{j \in \{0, \dots, N-1\}}$  is a sequence of i.i.d. zero-mean Gaussian variables with  $\mathbb{V}ar(\varepsilon_{j,N}) = 1/N$ . (2.3) yields the simulation of  $(B(1/N), \dots, B(1))$ .

For simulating discretized trajectories of fractional Brownian motion  $\{B^H(t)\}_{t \in [0,1]}$  with  $H \neq 1/2$ , we face the challenge of simulating correlated Gaussian random vectors. Multiple approaches have been suggested to address this challenge.

**Cholesky's decomposition-based method :** This method is often used in a general approach to simulate a Gaussian vector (process). Let  $\mathbb{N} = \{0, 1, 2, \dots\}$ . Assume that a discretized Gaussian process  $\{G(k)\}_{k \in \mathbb{N}}$  has covariance function

$$\gamma_{i,j} = \mathbb{C}ov(G(i), G(j)), \text{ for } i, j \in \mathbb{N}.$$

Then, for any time index  $n \in \mathbb{N}$ , given  $(G(0), \dots, G(n))$ , the conditional distribution of  $G(n+1)$  is also Gaussian with its mean and variance specified below:

$$\begin{aligned} & G(n+1) | (G(0), \dots, G(n)) \\ & \sim \mathcal{N} \left( C(n)^T M(n)^{-1} \begin{pmatrix} G(0) \\ \vdots \\ G(n) \end{pmatrix}, \gamma_{n+1,n+1} - C(n)^T M(n)^{-1} C(n) \right), \end{aligned} \quad (2.4)$$

where

- The column matrix  $C(n) = \begin{pmatrix} \gamma_{n+1,0} \\ \vdots \\ \gamma_{n+1,n} \end{pmatrix}$ .
- $M(n)$  is the covariance matrix of  $(G(0), \dots, G(n))$ , it satisfies the following recursion: for  $n \geq 0$ ,

$$M(n+1) = \begin{pmatrix} M(n) & C(n) \\ C(n)^T & \gamma_{n+1,n+1} \end{pmatrix}.$$

The general method for simulating a Gaussian process is then:

$$\begin{cases} \text{Set } G(0) = x_0, \text{ where } x_0 \in \mathbb{R} \text{ is a given initial value;} \\ \text{For } k = 1, \dots, n, G(k) \text{ is simulated via the distribution in (2.4).} \end{cases} \quad (2.5)$$

Note that one has to compute  $C(n)^T M(n)^{-1}$  for each  $n \geq 1$  in this simulation method. Several Cholesky's decomposition-based implementation methods are therefore suggested to compute this term, see [37, 38, 39, 20]. We point out that this general simulation approach applies to the simulation of fractional Brownian motion with covariance function (2.2).

**Fast Fourier transformation-based method :** Since fractional Brownian motion is a stationary increments Gaussian process, we can alternatively apply Davies and Harte's method [14] for simulating it. The implementation relies on the fast Fourier transformation. Let the auto-covariance function of the increments of fractional Brownian motion be given by

$$\gamma_H\left(\frac{k}{n}\right) = \text{Cov}\left(B^H\left(\frac{k+1}{n}\right) - B^H\left(\frac{k}{n}\right), B^H\left(\frac{1}{n}\right)\right).$$

We adjust Davies and Harte's [14] algorithm to simulate the fractional Brownian motion  $\{B^H(t)\}_{t \in [0,1]}$  below:

---

**Algorithm 1:** Simulation of fractional Brownian motion via the fast Fourier transform.

---

**Input:** *path length*  $n$ ; *auto-covariance function*  $\gamma_H$ .

- 1 **for**  $k = 1, \dots, 2n - 2$  **do**
- 2      $\alpha_k \leftarrow \frac{2\pi(k-1)}{2n-2}$ ;
- 3      $f_k \leftarrow \max \left\{ \text{Re} \left( \sum_{j=1}^{n-1} \gamma_H\left(\frac{j-1}{n}\right) e^{i(j-1)\alpha_k/n} + \sum_{j=n}^{2n-2} \gamma_H\left(\frac{2n-j-1}{n}\right) e^{i(j-1)\alpha_k/n} \right), 0 \right\}$ ;
- 4 **end**
- 5  $V_1 \leftarrow 0$ ;
- 6  $V_n \leftarrow 0$ ;
- 7 *Simulate independent zero-mean Gaussian variables*  $(U_1, \dots, U_n)$  *and*  $(V_2, \dots, V_{n-1})$  *with*
- 8  $\text{Var}(U_1) = \mathbb{V}\text{ar}(U_n) = 2$ ;
- 9  $\text{Var}(U_k) = \mathbb{V}\text{ar}(V_k) = 1$  for  $k \neq 1, n$ ;
- 10 **for**  $k = 1, \dots, n$  **do**
- 11      $Z_k \leftarrow U_k + iV_k$ ;
- 12 **end**
- 13 **for**  $k = n + 1, \dots, 2n - 2$  **do**
- 14      $Z_k \leftarrow U_{2n-k} - iV_{2n-k}$ ;
- 15 **end**
- 16 **for**  $t = 1, \dots, n$  **do**
- 17      $Y_t \leftarrow \frac{1}{2\sqrt{n-1}} \sum_{k=1}^{2n-2} \sqrt{f_k} e^{i(t-1)\alpha_k/n} Z_k$ ;
- 18 **end**
- 19 **for**  $t = 1, \dots, n$  **do**
- 20      $B^H\left(\frac{t}{n}\right) \leftarrow \sum_{k=1}^t Y_k$ ;
- 21 **end**

**Output:**  $(B^H(1/n), B^H(2/n), \dots, B^H(1))$ .

---

The notation  $\text{Re}(\bullet)$  denotes the real part of a complex value. The advantage of this method is that one can use the fast Fourier transform to efficiently compute  $f_k$  and  $Y_t$ . Moreover, Line 3 guarantees that  $f_k \geq 0$ , because the square root operator of  $f_k$  will be needed in the computa-

tion of  $Y_t$  in Line 17. Because of inherent computational error, it happens that  $f_k = 0$  for some  $k$ , which subsequently underestimates the covariances of the increments of fractional Brownian motion. Therefore, this fast Fourier transform method carries the risk of destroying the long-memory property of fractional Brownian motion. This issue has been mentioned in [2, 20] and is caused by the fact that the positivity condition for  $f_k$  is not always satisfied. Inspired by the simulation procedure in [14], [51] have proposed the circulant embedding approach for simulating stationary Gaussian random fields. In this latter framework, the positivity condition issue is addressed through “treating the dimension of the circulant as an integer parameter that is chosen to ensure that the circulant is positive definite”. To elaborate, Algorithm 1 applies the fast Fourier transform on the so-called Toeplitz matrix

$$T = \begin{pmatrix} \gamma_H(0) & \gamma_H\left(\frac{1}{n}\right) & \cdots & \gamma_H\left(\frac{n-1}{n}\right) \\ \gamma_H\left(\frac{1}{n}\right) & \gamma_H(0) & \cdots & \gamma_H\left(\frac{n-2}{n}\right) \\ \vdots & \vdots & \ddots & \vdots \\ \gamma_H\left(\frac{n-1}{n}\right) & \gamma_H\left(\frac{n-2}{n}\right) & \cdots & \gamma_H(0) \end{pmatrix}.$$

Note that  $T$  is not necessarily non-negative definite. Therefore, [51] suggest to embed  $T$  in a circulant covariance matrix

$$C = \begin{pmatrix} c_0 & c_1 & \cdots & c_{m-1} \\ c_{m-1} & c_0 & \cdots & c_{m-2} \\ \vdots & \vdots & \ddots & \vdots \\ c_1 & c_2 & \cdots & c_0 \end{pmatrix},$$

where  $m \geq 2(n-1)$  is some integer and

$$c_j = \begin{cases} \gamma_H\left(\frac{j}{m}\right) & \text{if } 0 \leq j \leq \frac{m}{2}; \\ \gamma_H\left(\frac{m-j}{m}\right) & \text{if } \frac{m}{2} < j \leq m-1. \end{cases}$$

Next, [51] suggest either to increase  $m$  or use the non-negative definite part of  $C$  in order to match the positivity condition.

**Moving average stochastic integral representation method :** Recall that the fractional Brownian motion can be equivalently defined via the moving average integral representation [49]:

$$B^H(t) = C_H \int_{-\infty}^t \left( (t-u)^{H-1/2} - \max(-u, 0)^{H-1/2} \right) dB(u), \quad (2.6)$$

where the constant  $C_H$  is chosen such that  $\mathbb{V}ar(B^H(1)) = 1$ :

$$C_H = \left\{ \int_{-\infty}^0 \left( (t-u)^{H-1/2} - (-u)^{H-1/2} \right)^2 du + \frac{1}{2H} \right\}^{-1/2}.$$

Based on (2.6), one can use the truncation method to simulate a discrete path of fractional Brownian motion. However, since the stochastic integral (2.6) is indefinite, the truncation might also destroy the long-memory property [20].

**Series representation methods :** There exist other simulation methods based on representation results of fractional Brownian motion. For example, the representation of fractional Brownian motion in Theorem 5.2 given in [41] does not require truncation. Therefore, the long-memory property is preserved by the simulation method based on the following integral representation:

$$B^H(t) = \int_0^t z(t, s) dW(s),$$

where  $\{W(s)\}_{s \geq 0}$  is a standard Brownian motion and

$$\begin{aligned} z(t, z) &= \left( \frac{2H\Gamma(3/2 - H)}{\Gamma(H + 1/2)\Gamma(2 - 2H)} \right)^{1/2} \\ &\times \left( \left( \frac{t}{s} \right)^{H-1/2} (t-s)^{H-1/2} - (H - \frac{1}{2})s^{1/2-H} \int_s^t u^{H-3/2} (u-s)^{H-1/2} du \right). \end{aligned}$$

For fractional Brownian motion with the long-memory property ( $H > 1/2$ ), we can simplify the above expression to

$$z(t, s) = \left( \frac{2H\Gamma(3/2 - H)}{\Gamma(H + 1/2)\Gamma(2 - 2H)} \right)^{1/2} {}_2F_1 \left( \frac{1}{2} - H, H - \frac{1}{2}, H + \frac{1}{2}, 1 - \frac{t}{s} \right),$$

where  ${}_2F_1$  is the Gauss hypergeometric function. Finally, there exist alternative simulation methods based on wavelet representations. For example, a mean-square sense wavelet representation of fractional Brownian motion is given in [21], where, for any given resolution  $2^J$  with  $J \in \mathbb{Z}$ ,

$$B^H(t) = 2^{-J/2} \sum_{n=-\infty}^{+\infty} a_{J,n} \phi(2^{-J}t - n) + \sum_{j=-\infty}^J 2^{-j/2} \sum_{n=-\infty}^{+\infty} d_{j,n} \psi(2^{-j}t - n),$$

where  $\psi(t)$  is the basic wavelet function and  $\phi(t)$  is the scaling function associated to  $\psi(t)$  [35]; the approximation coefficients are

$$\begin{aligned} a_{j,n} &= 2^{-j/2} \int_{-\infty}^{+\infty} B^H(t) \phi(2^{-j}t - n) dt; \\ d_{j,n} &= 2^{-j/2} \int_{-\infty}^{+\infty} B^H(t) \psi(2^{-j}t - n) dt. \end{aligned}$$

There exist other wavelet representations of fractional Brownian motion, for example, in [50, 1, 13]. The wavelet decomposition methods may suffer from accuracy, high complexity issues, and the destruction of the long-memory property.

In conclusion, so far, the most promising method for simulating fractional Brownian motion stems from [51], thanks to the fact that the method does not destroy the long-memory property and is relatively accurate and efficient.

For simulating other self-similar Gaussian processes very similar to fractional Brownian motion, such as fractional Gaussian noise and fractional ARIMA, we refer the readers to [8, 18]. Murad Taqqu's website <http://math.bu.edu/people/murad> offers great insight on simulation strategies for self-similar processes [20].

Some real-world data also display self-similar and light-tail properties, such as fractional teletraffic data. Simulating these types of data plays an important role in both industrial settings and academic research. Various methods have been suggested to simulate them and are more or less inspired by those for simulating fractional Brownian motion; see the FGN-DW methods in [24, 26, 25].

### 3 Simulation of Multifractional Brownian Motion

Multifractional Brownian motion, as one of the most natural extensions of fractional Brownian motion, is a continuous-time Gaussian process with a time-dependent self-similarity parameter. It is not self-similar but locally asymptotically self-similar [7, 11]. Unlike fractional Brownian motion, multifractional Brownian motion has non-stationary increments when its Hurst functional parameter is not a constant. In the literature, multifractional Brownian motion has been introduced separately and independently by both [33] and [7]. In [33], multifractional Brownian motion can be defined via the moving-average representation

$$X^{(1)}(t) = \int_{-\infty}^{+\infty} \left( (t-u)_+^{H(t)-1/2} - (-u)_+^{H(t)-1/2} \right) dW(u), \quad (3.1)$$

where we denote  $(x)_+ = \max\{x, 0\}$  for any real number  $x$ , the function  $H$  is continuous, taking values in  $(0, 1)$ , and  $dW(u)$  denotes an independently scattered standard Gaussian measure on  $\mathbb{R}$ . In [7], multifractional Brownian motion is defined via the so-called harmonizable integral representation as

$$X^{(2)}(t) = \int_{-\infty}^{+\infty} \frac{e^{it\xi} - 1}{|\xi|^{H(t)+1/2}} d\widetilde{W}(\xi), \quad (3.2)$$

where  $d\widetilde{W}(\xi)$  denotes a complex-valued Gaussian measure. Note that the two definitions (3.1) and (3.2) have different covariance structures due to different scaling coefficients [46]. In this paper, we discuss only simulation methods of the multifractional Brownian motion  $X(t)$  defined by [12], which is a modification of  $X^{(1)}(t)$ . Simulations of both  $X^{(1)}(t)$  and  $X^{(2)}(t)$  can be obtained from simple adjustments.

Recall that the version of the multifractional Brownian motion considered in [12] is the following:

$$X(t) = \widetilde{C}(H) \int_{-\infty}^{+\infty} (1 - \cos(st) - \sin(st)) |s|^{-H-1/2} dW(s),$$

where  $\widetilde{C}(H)$  is a real-valued function such that  $\text{Var}(X(t)) = |t|^{2H}$ , and  $W$  is a standard Brownian motion.  $X(t)$  has the covariance function: for  $s, t \geq 0$ ,

$$\text{Cov}(X(s), X(t)) = \frac{g(H(s), H(t))}{2} \left( |s|^{H(s)+H(t)} + |t|^{H(s)+H(t)} - |t-s|^{H(s)+H(t)} \right), \quad (3.3)$$

where for  $H_1, H_2, H \in (0, 1)$ ,  $g(H_1, H_2) = (I(H_1)I(H_2))^{-1/2} I((H_1 + H_2)/2)$  and

$$I(H) = \begin{cases} \frac{\Gamma(1-2H)}{H} \sin\left(\frac{(1-2H)\pi}{2}\right) & \text{for } H \in (0, 1/2); \\ \pi & \text{for } H = 1/2; \\ \frac{\Gamma(2(1-H))}{H(2H-1)} \sin\left(\frac{(2H-1)\pi}{2}\right) & \text{for } H \in (1/2, 1). \end{cases}$$

The main simulation approaches provided by the literature consist of Wood-Chan's method [12] and wavelet-based simulations [5, 27].

We summarize Wood-Chan's algorithm [12] to simulate the multifractional Brownian motion  $\{X(t)\}_{t \in [0,1]}$  below:

---

**Algorithm 2:** Simulation of multifractional Brownian motion via FFT.

---

**Input:** the path length  $n$ ; the discretized Hurst functional parameter  $H_{1/(m+1)}, \dots, H_{m/(m+1)}$ .

- 1 **for**  $u = 1, \dots, m$  **do**
- 2     **for**  $j = 1, \dots, n$  **do**
- 3         Simulate  $Y_{j,u}$  using the circulant embedding approach for stationary vector-valued Gaussian processes via the covariance function (see (3.3)):
- 4         
$$\text{Cov}(Y_{j,u}, Y_{k,v}) = \frac{g(H_u, H_v)}{2} (|j - k - 1|^{H_u + H_v} + |j - k + 1|^{H_u + H_v} - 2|j - k|^{H_u + H_v});$$
- 5     **end**
- 6     **for**  $u = 1, \dots, m$  **do**
- 7         **for**  $j = 1, \dots, n$  **do**
- 8              $Z_{j,u} \leftarrow n^{H_u} \sum_{k=1}^j Y_{k,u};$
- 9         **end**
- 10     **end**
- 11     **for**  $j = 1, \dots, n$  **do**
- 12         Simulate  $X_{j/n}$  using some form of kriging based on the observations  $\{Y_{j,u}\}_{j \in \{1, \dots, n\}, u \in \{1, \dots, m\}}$ :
- 13         
$$N_j \leftarrow \{j - q, \dots, j + q\} \times \{[mH_{j/n}] - q, \dots, [mH_{j/n}] + q\} \cap \{1, \dots, n\} \times \{1, \dots, m\};$$
- 14         
$$X(j/n) \leftarrow \sum_{(k,v) \in N_j} \text{Cov}((Z_{k,v})_{(k,v) \in N_j})^{-1} \text{Cov}((Z_{k,v})_{(k,v) \in N_j}, Z_{j,j}) Z_{k,v};$$
- 15     **end**

**Output:** A sample path  $(X(1/n), X(2/n), \dots, X(1))$ .

---

Note that in Lines 12 - 13 of Algorithm 2, each  $X(j/n)$  is evaluated by minimizing the variance of  $X(j/n) - \sum_{(k,v) \in N_j} \beta_{k,v} Z_{k,v}$  with respect to  $\beta_{k,v}$ . The optimizer is given as

$$\hat{\beta}_{k,v} = \text{Cov}((Z_{k,v})_{(k,v) \in N_j})^{-1} \text{Cov}((Z_{k,v})_{(k,v) \in N_j}, Z_{j,j}),$$

where the covariance matrices

$$\text{Cov}((Z_{k,v})_{(k,v) \in N_j}) = \mathbb{E} \left\{ (Z_{k,v})_{(k,v) \in N_j}^T (Z_{k,v})_{(k,v) \in N_j} \right\}$$

and

$$\text{Cov}((Z_{k,v})_{(k,v) \in N_j}, Z_{j,j}) = \mathbb{E} \left\{ Z_{j,j} (Z_{k,v})_{(k,v) \in N_j} \right\}.$$

The right-hand sides of the above two equations are computed using the covariance function (3.3).

Since Algorithm 2 uses Wood and Chan's circulant embedding method [51], it therefore avoids ruining the long-memory property of the locally asymptotical self-similarity of multifractional Brownian motion. Algorithm 2 itself works, and its implementation in MATLAB can be found in FracLab (<https://project.inria.fr/fraclab/>). However, we have found that this implementation of the fractional Brownian random field  $Y_{j,u}$ ,  $(j, u) \in \{1, \dots, n\} \times \{1, \dots, m\}$  given in Line 3 is only approximative and does not follow the approach for simulating a Gaussian random field given in [51]. In fact, the implementation in FracLab assumes that the vectors  $(Y_{1,u}, \dots, Y_{n,u})$  are independent with respect to  $u \in \{1, \dots, m\}$ , although they are not. This assumption, together with Line 12 introduces more bias than Wood-Chan's method for simulating fractional Brownian motions. So far, we have

not yet found a resource that exactly implements Algorithm 2. To conclude, there is still space to improve the accuracy of Wood-Chan's method for simulating multifractional Brownian motion.

Other simulation methods include the moving-average stochastic integral representation method [33] and Wavelet-based decomposition methods [3, 15]. Similarly to the approaches proposed for simulating fractional Brownian motion, these approaches have pros and cons. While the moving-average stochastic integral representation method truncates the integral and destroys long-range dependency, wavelet-based methods are largely inefficient and inaccurate.

## 4 Simulation of Self-similar Processes with Non-stationary Increments

The well-known fractional Brownian motion has stationary increments. [51] have taken advantage of this feature to simulate fractional Brownian motion and multifractional Brownian motion. However, not all self-similar processes exhibit this property. Examples include sub-fractional Brownian motion [10], bi-fractional Brownian motion [23], and tri-fractional Brownian motion [34]. In these cases, Wood and Chan's methods no longer work. We take the sub-fractional Brownian motion as an example below.

The sub-fractional Brownian motion (sfBm for short)  $\{S^H(t)\}_{t \geq 0}$  is a centered Gaussian self-similar process with  $S^H(0) = 0$  and covariance function: for  $s, t \geq 0$ ,

$$\text{Cov}(S^H(t), S^H(s)) = t^{2H} + s^{2H} - \frac{1}{2}((t+s)^{2H} + |t-s|^{2H}), \quad (4.1)$$

with the parameter  $H \in (0, 1)$ . For sub-fractional Brownian motion, the existing simulation methods consist of some variants of the moving-average integral representations [40, 29]. Like other integral representation methods, the simulation approaches in [40] and [29] suffer from truncation or approximation problems.

For bi-fractional Brownian motion and tri-fractional Brownian motion which have neither non-stationary increments nor simple integral representations, we have not found any study on the simulation of these two processes in the literature, showcasing the complexity of researching and simulating self-similar processes. In Section 6, we will shed some light on this problem by introducing a brand new simulation methodology.

## 5 Simulation of Linear Fractional Stable Motion

In this section, we investigate the simulation of self-similar non-Gaussian processes. A typical example is linear fractional stable motion (LFSM), introduced in [44]. Recall that the linear fractional stable motion  $\{X(t)\}_{t \in \mathbb{R}}$  with the tail-heaviness control parameter (also called stability parameter)  $\alpha \in (0, 2)$  and the Hurst parameter (also called self-similarity parameter)  $H \in (0, 1)$  [4] is defined as follows: on a filtered probability space  $(\Omega, \mathcal{F}, (\mathcal{F}_t)_{t \geq 0}, \mathbb{P})$ ,

$$X(t) = \int_{\mathbb{R}} g_H(t, s) dM_{\alpha}(s), \text{ for } t \in \mathbb{R}, \quad (5.1)$$

where:

(1) In the kernel

$$g_H(t, s) = \kappa \left\{ (t-s)_+^{H-1/\alpha} - (-s)_+^{H-1/\alpha} \right\}, \quad (5.2)$$

$\kappa > 0$  is a normalizing constant such that the scale parameter of  $X(1)$ , denoted by  $\|X(1)\|_\alpha = (\int_{\mathbb{R}} |g_H(1, s)|^\alpha ds)^{1/\alpha}$ , equals 1; we employ the convention  $0^{H-1/\alpha} = 0$  for all  $H \in (0, 1)$  and  $\alpha \in (0, 2)$ .

(2)  $M_\alpha$  is a strictly  $\alpha$ -stable random measure on  $\mathbb{R}^N$  with Lebesgue measure as its control measure and with  $\beta(s)$  as its skewness intensity (see [44]). That is, for every Lebesgue measurable set  $E \subset \mathbb{R}^N$  with Lebesgue measure  $\lambda(E) < +\infty$ ,  $M_\alpha(E)$  is a strictly  $\alpha$ -stable random variable with scale parameter  $\sigma = \lambda(E)^{1/\alpha}$  and skewness parameter  $\beta = (1/\lambda(E)) \int_E \beta(s) ds$ . More precisely, the characteristic function of  $M_\alpha(E)$  has the following form (see Definition 1.1.6, [44]): for  $x \in \mathbb{R}$ ,

$$\mathbb{E} \left[ e^{ixM_\alpha(E)} \right] = \begin{cases} \exp \{ -\sigma^\alpha |x|^\alpha (1 - i\beta(\text{sign}(x)) \tan(\pi\alpha/2)) \} & \text{if } \alpha \neq 1; \\ \exp \{ -\sigma |x| (1 + 2i\beta \text{sign}(x) \log(|x|)/\pi) \} & \text{if } \alpha = 1, \end{cases}$$

where

$$\text{sign}(x) = \begin{cases} 1 & \text{if } x > 0; \\ 0 & \text{if } x = 0; \\ -1 & \text{if } x < 0. \end{cases}$$

We also denote  $M_\alpha(E) \sim S_\alpha(\sigma, \beta)$ . If  $\beta(\bullet) \equiv 0$ ,  $M_\alpha$  becomes a symmetric  $\alpha$ -stable random measure. In this case,  $M_\alpha(E) \sim S_\alpha(\sigma, 0)$ , i.e.,

$$\mathbb{E} \left[ e^{ixM_\alpha(E)} \right] = \exp \{ -\sigma^\alpha |x|^\alpha \} \text{ for } \alpha \in (0, 2).$$

The special convention  $0^{H-1/\alpha} = 0$  in (5.2) yields that, when  $H = 1/\alpha$ , LFSM becomes the ordinary stable sheet. When  $\alpha = 2$ , LFSM becomes fractional Brownian motion.

Since LFSM is non-Gaussian, the simulation approaches based on the moments, such as Cholesky's decomposition and the circulant embedding methods, do not apply anymore. The existing simulation methods are through integral representations and the Fourier series decomposition method. The integral representation methods were introduced in [45]. This method directly truncates the integral in (5.1). [52] approximate the integral (5.1) based on a linear process. [9] use the Fourier series representation of LFSM to simulate it.

## 6 A Modified Inverse Lamperti Transformation Approach

In this section, we develop a novel method to simulate a zero-mean Gaussian self-similar process. Our simulation methodology involves using a modified inverse Lamperti transformation, which transforms self-similar processes to stationary ones. We will take the simulation of fractional Brownian motions and sub-fractional Brownian motions as examples, but point out that this new idea has the potential to be generalized to simulate a much larger class of self-similar processes.

Based on the above investigation of the existing simulation approaches, we believe that working on the transformation of self-similar processes to stationary processes may point in the direction of an efficient generating algorithm of self-similar processes. Therefore, the Lamperti transformation [30] can be applied. The Lamperti transformation of a stationary process  $\{Y(t)\}_{t \geq 0}$  is defined to be

$$X(t) = t^H Y(\log(t)), \text{ for } t > 0 \text{ and some } H \in (0, 1).$$

The Lamperti transformation with parameter  $H$  transforms a stationary process to a self-similar process with self-similarity parameter  $H$ . Its inverse hence transforms a self-similar process back to

a stationary process. The inverse Lamperti transformation of a self-similar process  $\{X(t)\}_{t \geq 0}$  with self-similarity parameter  $H \in (0, 1)$  is thus given by

$$Y(t) = e^{-Ht} X(e^t), \text{ for } t \geq 0.$$

Since  $\{Y(t)\}_{t \geq 0}$  is stationary, the simulation of  $\{X(t)\}_{t \geq 0}$  can be obtained through the simulation of  $\{Y(t)\}_{t \geq 0}$ , which is much simpler. This idea may provide hope for developing a general method for simulating self-similar processes.

By using the Lamperti transformations, we suggest the following novel method to simulate a zero-mean Gaussian self-similar process  $\{X(t)\}_{t \in [0,1]}$ :

1. Given the length  $n \geq 1$ , use Wood-Chan's method [51] to simulate a sample path of the stationary Gaussian process

$$U\left(\frac{k}{n}\right) = n^{-H(k/n-1)} X(n^{k/n-1}), \text{ for } k = 1, \dots, n \quad (6.1)$$

via its autocovariance function

$$\gamma_U\left(\frac{k}{n}\right) = \mathbb{C}ov\left(U\left(\frac{1}{n}\right), U\left(\frac{k+1}{n}\right)\right). \quad (6.2)$$

2. For  $j = 1, \dots, n$ , take

$$\tilde{X}\left(\frac{j}{n}\right) = \left(\frac{j}{n}\right)^H U\left(\frac{\lfloor\left(\frac{\log(j/n)}{\log n} + 1\right)n\rfloor}{n}\right), \quad (6.3)$$

where  $\lfloor \bullet \rfloor$  denotes the floor number.

We explain how the above algorithm works. (6.1) is a modified version of the inverse Lamperti transformation of  $\{X(t)\}_{t \in [0,1]}$ , where the mapping  $t \mapsto n^{t-1}$  is a bijection from  $[0, 1]$  to  $[1/n, 1]$ . This mapping allows one to transform  $(U(1/n), \dots, U(1))$  back to  $(X(1/n), \dots, X(1))$ . By (6.1), we get

$$\begin{aligned} \left(\tilde{X}\left(\frac{j}{n}\right)\right)_{j=1, \dots, n} &= \left(\left(\frac{j}{n}\right)^H U\left(\frac{\lfloor\left(\frac{\log(j/n)}{\log n} + 1\right)n\rfloor}{n}\right)\right)_{j=1, \dots, n} \\ &= \left(\left(\frac{j}{n}\right)^H n^{-H\left(\frac{\lfloor\left(\frac{\log(j/n)}{\log n} + 1\right)n\rfloor}{n} - 1\right)} X\left(n^{\lfloor\left(\frac{\log(j/n)}{\log n} + 1\right)n\rfloor - 1}\right)\right)_{j=1, \dots, n} \\ &= \left(\left(\frac{j}{n}\right)^H n^{-H\left(\frac{(\log(j/n) + 1)n - \theta_{j,n}}{n} - 1\right)} X\left(n^{\frac{(\log(j/n) + 1)n - \theta_{j,n}}{n} - 1}\right)\right)_{j=1, \dots, n} \\ &= \left(n^{H\theta_{j,n}/n} X\left(\frac{j}{n} \cdot n^{-\theta_{j,n}/n}\right)\right)_{j=1, \dots, n}, \end{aligned} \quad (6.4)$$

where

$$\theta_{j,n} = \left(\frac{\log(j/n)}{\log n} + 1\right)n - \left\lfloor\left(\frac{\log(j/n)}{\log n} + 1\right)n\right\rfloor \in (0, 1) \text{ for } j \in \{1, \dots, n\}. \quad (6.5)$$

Then  $(\tilde{X}(j/n))_{j=1, \dots, n}$  are “good” approximations of  $(X(j/n))_{j=1, \dots, n}$  in the following sense:

(i) By the self-similarity, we see that

$$\tilde{X}\left(\frac{j}{n}\right) \stackrel{\text{law}}{=} X\left(\frac{j}{n}\right) \text{ for each } j \in \{1, \dots, n\}. \quad (6.6)$$

This means that the marginal distributions of  $(\tilde{X}(j/n))_{j=1, \dots, n}$  and  $(X(j/n))_{j=1, \dots, n}$  are equal. However, their joint distributions are in general distinct.

(ii) Assume that the sample paths of  $\{X(t)\}_{t \in [0,1]}$  are almost surely Hölder continuous with Hölder's index  $\beta \in (0, 1)$ , i.e., there is a positive random variable  $C$  such that

$$\sup_{s, t \in [0,1]} |X(s) - X(t)| \leq C|s - t|^\beta \text{ a.s..} \quad (6.7)$$

Then by the triangle inequality and (6.7), for any  $j \in \{1, \dots, n\}$ ,

$$\begin{aligned} & \left| n^{H\theta_{j,n}/n} X\left(\frac{j}{n} \cdot n^{-\theta_{j,n}/n}\right) - X\left(\frac{j}{n}\right) \right| \\ & \leq \left| n^{H\theta_{j,n}/n} - 1 \right| \left| X\left(\frac{j}{n} \cdot n^{-\theta_{j,n}/n}\right) \right| + \left| X\left(\frac{j}{n} \cdot n^{-\theta_{j,n}/n}\right) - X\left(\frac{j}{n}\right) \right| \\ & \leq \left( \sup_{s \in [0,1]} |X(s)| \right) \left| n^{H\theta_{j,n}/n} - 1 \right| + C \left( \frac{j}{n} \right)^{\beta-\varepsilon} \left| n^{-\theta_{j,n}/n} - 1 \right|^\beta. \end{aligned}$$

By the mean value theorem and the fact that  $\lim_{n \rightarrow +\infty} n^{1/n} = 1$ , there is a constant  $c_1 > 0$  which does not depend on  $j$  nor on  $n$ , such that

$$\left| n^{H\theta_{j,n}/n} - 1 \right| = \left| \left( n^{1/n} \right)^{H\theta_{j,n}} - \left( n^{1/n} \right)^0 \right| = \frac{(n^{1/n})^{\eta_{j,n}} \log(n)}{n} H\theta_{j,n} \leq c_1 \frac{\log(n)}{n},$$

where  $\eta_{j,n}$  is some value in  $(0, H\theta_{j,n}) \subset (0, H)$  for any  $n \geq 1$  and  $j \in \{1, \dots, n\}$ . In the same way, there is a constant  $c_2 > 0$  which does not depend on  $j$  nor on  $n$ , such that

$$\left| n^{-\theta_{j,n}/n} - 1 \right| \leq c_2 \frac{\log(n)}{n}.$$

It follows that, for any  $j \in \{1, \dots, n\}$ ,

$$\left| n^{H\theta_{j,n}/n} X\left(\frac{j}{n} \cdot n^{-\theta_{j,n}/n}\right) - X\left(\frac{j}{n}\right) \right| \leq \tilde{C} n^{-\beta} (\log(n))^\beta, \quad (6.8)$$

where the random variable  $\tilde{C} = c_1 \sup_{s \in [0,1]} |X(s)| + c_2 C$  does not depend on  $j$  nor on  $n$ . Finally, (6.8) together with (6.4) yields

$$\max_{j \in \{1, \dots, n\}} \left| \tilde{X}\left(\frac{j}{n}\right) - X\left(\frac{j}{n}\right) \right| \leq \tilde{C} n^{-\beta} (\log(n))^\beta \xrightarrow[n \rightarrow +\infty]{a.s.} 0. \quad (6.9)$$

We know that  $\{X(t)\}_{t \in [0,1]}$  is a Gaussian process. If all its sample paths are almost surely continuous, then by applying Dudley's theorem and Borell's inequality (see Pages 1445-1446 in [42], see also [32]), we can show that any order moments of  $\sup_{s \in [0,1]} |X(s)|$  and  $C$  are finite. These facts together with (6.9) imply that

$$\mathbb{E} \left( \max_{j \in \{1, \dots, n\}} \left| \tilde{X}\left(\frac{j}{n}\right) - X\left(\frac{j}{n}\right) \right| \right)^2 \leq c n^{-2\beta} (\log(n))^{2\beta}, \quad (6.10)$$

where  $c = \mathbb{E} |\tilde{C}|^2 < +\infty$ .

## 6.1 Application I: Simulation of Fractional Brownian Motion

The modified inverse Lamperti transformation approach can be applied to simulate sample paths of a fractional Brownian motion  $\{B^H(t)\}_{t \in [0,1]}$ , defined via (2.2). It suffices to note that

$$\begin{aligned}\gamma_U \left( \frac{k}{n} \right) &= \mathbb{C}ov \left( n^{-H(1/n-1)} B^H(n^{1/n-1}), n^{-H((k+1)/n-1)} B^H(n^{(k+1)/n-1}) \right) \\ &= \frac{1}{2} n^{-H((k+2)/n-2)} \left( n^{2H(1/n-1)} + n^{2H((k+1)/n-1)} - \left| n^{1/n-1} - n^{(k+1)/n-1} \right|^{2H} \right) \\ &= \frac{1}{2} \left( n^{-Hk/n} + n^{-Hk/n} - \left| n^{-k/(2n)} - n^{-k/(2n)} \right|^{2H} \right), \text{ for } k = 1, \dots, n\end{aligned}\quad (6.11)$$

in the simulation algorithm (6.1) - (6.3). As the fractional Brownian motion is a Gaussian process having almost surely Hölder continuous sample paths with the Hölder index  $H - \varepsilon$  for any  $\varepsilon > 0$  arbitrarily small, the error analysis results (6.6) - (6.10) hold with  $\beta = H - \varepsilon$ . We summarize the pseudocode for simulating  $\{B^H(t)\}_{t \in [0,1]}$  below:

---

**Algorithm 3:** Simulation of a discrete sample path of the fractional Brownian motion  $(B^H(1/n), B^H(2/n), \dots, B^H(1))$ .

---

**Input:** the path length  $n$ ; the Hurst parameter  $H$ ; the covariance function  $\gamma_U$  given in (6.11).

1 Use Wood-Chan's method [51] to simulate a sample path of  $U$  based on its autocovariance function  $\gamma_U$ :

2  $U \leftarrow \{U(1/n), U(2/n), \dots, U(1)\}$ ;

3 Simulate  $(B^H(1/n), B^H(2/n), \dots, B^H(1))$ :

4 for  $j = 1, \dots, n$  do

5  $B^H(\frac{j}{n}) \leftarrow (\frac{j}{n})^H U \left( \left\lfloor \frac{(\frac{\log(j/n)}{\log n} + 1)n}{n} \right\rfloor \right)$ ;

6 end

**Output:** A sample path  $(B^H(1/n), B^H(2/n), \dots, B^H(1))$ .

---

Algorithm 3 has been implemented in the Python library “fractal analysis” (<https://pypi.org/project/fractal-analysis/>) by Yujia Ding. The above Python library also implements [6]’s approach for the hypothesis test of fractional Brownian motion. The test tells whether the observed path is sampled from the fractional Brownian motion  $\{B^H(t)\}_{t \in [0,1]}$  with some given  $H$ . Using this test, we compare our algorithm to Wood-Chan’s method. We summarize the comparison results below:

Pass Rate of Balcerak and Burnecki's Hypothesis Test				
Hurst Parameter $H$	$\alpha = 5\%$		$\alpha = 1\%$	
	Wood-Chan	Algorithm 3	Wood-Chan	Algorithm 3
0.01	72.8%	97.8%	93.5%	99.9%
0.2	87.6%	100%	97.0%	100%
0.5	90.3%	99.8%	97.5%	100%
0.8	91.8%	99.5%	98.2%	100%
0.99	93.8%	99.4%	98.6%	100%

Table 1:  $\alpha$  is the significance level of the test. Each pass rate is obtained by testing 1000 simulated sample paths of  $(B^H(1/n), \dots, B^H(1))$  with length  $n = 1024$ .

Although the hypothesis test has its own testing errors, Table 1 shows that Algorithm 3 outperforms Wood-Chan's method in view of the pass rate. We also observe that the performance of Wood-Chan's method is not consistent with respect to the parameter  $H$ : greater is the value of  $H$ , greater is the pass rate. This is because Wood-Chan's method is based on simulating the increments of fractional Brownian motion,  $\{B^H((j+1)/n) - B^H(j/n)\}_{j=0, \dots, n-1}$ , which have higher variance when  $H$  is smaller. However, Algorithm 3 does not have such issue. Below we illustrate some sample paths simulated by Algorithm 3.

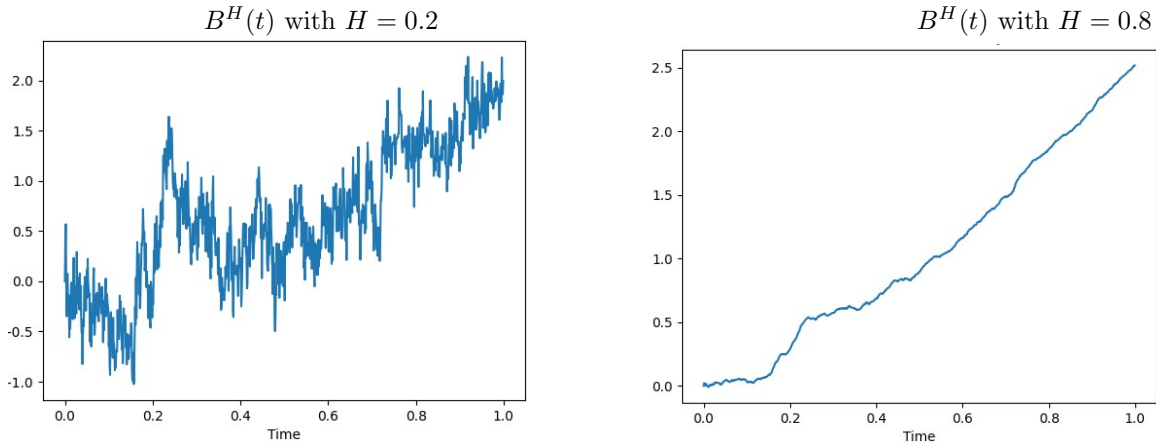


Figure 1: Sample paths of  $\{B^H(t)\}_{t \in [0,1]}$  simulated by using Algorithm 3.

From Figure 1, we see that the Hölder's regularity of the simulated sample paths indeed changes via the value of  $H$ .

## 6.2 Application II: Simulation of Sub-fractional Brownian Motion

Unlike fractional Brownian motion, the sub-fractional Brownian motion  $\{S^H(t)\}_{t \in [0,1]}$  defined in (4.1) has non-stationary increments, which makes Wood-Chan's method no longer work. However, the modified inverse Lamperti transformation method applies here. In the algorithm (6.1) - (6.3),

we take

$$\begin{aligned}
\gamma_U \left( \frac{k}{n} \right) &= \mathbb{C}ov \left( n^{-H(1/n-1)} S^H(n^{1/n-1}), n^{-H((k+1)/n-1)} S^H(n^{(k+1)/n-1}) \right) \\
&= n^{-H((k+2)/n-2)} \left( n^{2H(1/n-1)} + n^{2H((k+1)/n-1)} \right. \\
&\quad \left. - \frac{1}{2} \left( \left( n^{1/n-1} + n^{(k+1)/n-1} \right)^{2H} + \left| n^{1/n-1} - n^{(k+1)/n-1} \right|^{2H} \right) \right) \\
&= n^{-Hk/n} + n^{Hk/n} - \frac{1}{2} \left( (n^{-k/(2n)} + n^{k/(2n)})^{2H} + |n^{-k/(2n)} - n^{k/(2n)}|^{2H} \right), 
\end{aligned} \tag{6.12}$$

for  $k = 1, \dots, n$ . From the sub-fractional Brownian motion's covariance structure and the Kolmogorov-Čentsov theorem, we know that  $\{S^H(t)\}_{t \in [0,1]}$  is also a Gaussian process whose sample paths are almost surely  $(H - \varepsilon)$ -Hölder continuous for arbitrarily small  $\varepsilon > 0$ . Therefore, the error analysis results (6.6) - (6.10) hold with  $\beta = H - \varepsilon$  for the sub-fractional Brownian motion. We summarize the pseudocode for simulating  $\{S^H(t)\}_{t \in [0,1]}$  below:

---

**Algorithm 4:** Simulation of a discrete sample path of the sub-fractional Brownian motion  $(S^H(1/n), S^H(2/n), \dots, S^H(1))$ .

---

**Input:** *the path length n; the self-similarity index H; the covariance function  $\gamma_U$  given in (6.12).*

- 1 **Use Wood-Chan's method to simulate a sample path of U based on its autocovariance function  $\gamma_U$ :**
- 2  $U \leftarrow \{U(1/n), U(2/n), \dots, U(1)\}$ ;
- 3 **Simulate  $(S^H(1/n), S^H(2/n), \dots, S^H(1))$ :**
- 4 **for**  $j = 1, \dots, n$  **do**
- 5      $S^H(\frac{j}{n}) \leftarrow \left( \frac{j}{n} \right)^H U \left( \frac{\lfloor (\frac{\log(j/n)}{\log n} + 1)n \rfloor}{n} \right)$ ;
- 6 **end**

**Output:** A sample path  $(S^H(1/n), S^H(2/n), \dots, S^H(1))$ .

---

Algorithm 4 has also been implemented in the Python library “fractal analysis”. Since the test of sub-fractional Brownian motion has not yet been found in the literature, we only illustrate some sample paths simulated by Algorithm 4 below.

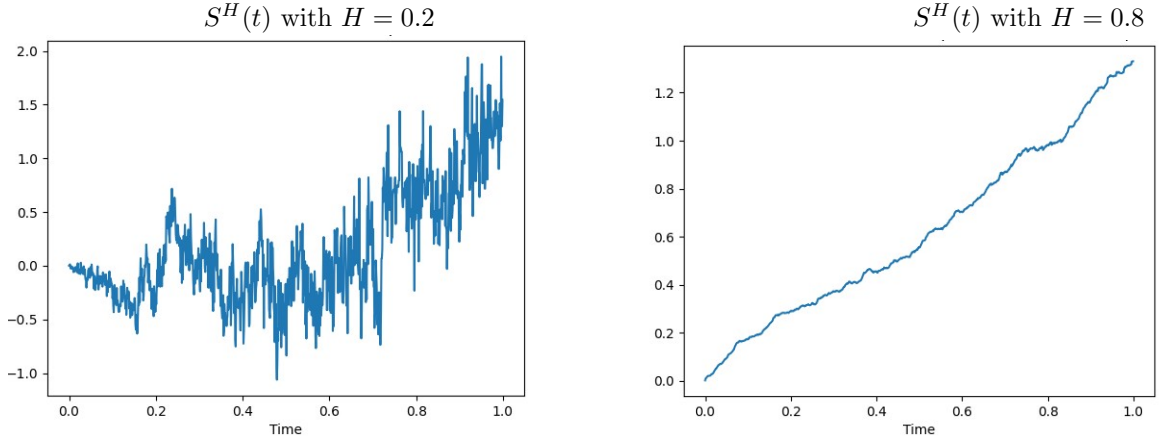


Figure 2: Sample paths of  $\{S^H(t)\}_{t \in [0,1]}$  simulated by using Algorithm 4.

Figure 2 supports the fact that the sub-fractional Brownian motion is self-similar with the self-similarity index  $H$ .

## 7 Conclusion

There is a growing body of research on various self-similar processes, including the introduction of new types of self-similar processes, studying their paths features, and developing statistical inference tools. There is not yet a promising methodology that can efficiently simulate their sample paths. For example, although bi-fractional Brownian motion and tri-fractional Brownian motion have been receiving growing attention, simulation methods have yet to be developed for them. The first goal of this paper then has been to illuminate a direction of research that aims to shed light on the development of general simulation strategies for the above self-similar processes. The prototypical examples we have chosen to investigate are fractional Brownian motion, sub-fractional Brownian motion, multifractional Brownian motion, and linear fractional stable motion. Based on the above investigation of the existing simulation approaches, we believe that working on the transformation of self-similar processes to stationary processes may point in the direction of an efficient generating algorithm of self-similar processes. Therefore, the Lamperti transformation is a potential powerful tool to be used to simulate a general self-similar process. We then have proposed a new method to simulate self-similar processes. This method uses a modified version of the inverse Lamperti transformation to transform the self-similar process to a stationary Gaussian process. Simulating the self-similar process is then equivalent to simulate the latter stationary process. The second contribution of this paper has been to successfully apply this novel method to simulate the fractional Brownian motion and sub-fractional Brownian motion. Comparison results show that our new method outperforms Wood-Chan's method via the hypothesis test pass rate. We believe that this idea can be further extended to simulate a large class of self-similar processes which are Gaussian processes with non-stationary increments or are non-Gaussian processes, including bi-fractional Brownian motion, tri-fractional Brownian motion, and linear fractional stable motion.

## Acknowledgment:

The authors thank Yujia Ding for helping to implement the simulation and testing algorithms in the Python library.

## References

- [1] S Albeverio, Palle ET Jorgensen, and Anna Maria Paolucci. On fractional Brownian motion and wavelets. *Complex Analysis and Operator Theory*, 6(1):33–63, 2012.
- [2] Søren Asmussen. *Stochastic Simulation with A View towards Stochastic Processes*. University of Aarhus. Centre for Mathematical Physics and Stochastics, 1998.
- [3] Antoine Ayache, Stéphane Jaffard, and Murad S Taqqu. Wavelet construction of generalized multifractional processes. *Revista Matemática Iberoamericana*, 23(1):327–370, 2007.
- [4] Antoine Ayache, François Roueff, and Yimin Xiao. Local and asymptotic properties of linear fractional stable sheets. *Comptes rendus. Mathématique*, 344(6):389–394, 2007.
- [5] Antoine Ayache, Narn-Rueih Shieh, and Yimin Xiao. Multiparameter multifractional Brownian motion: local nondeterminism and joint continuity of the local times. In *Annales de l'IHP Probabilités et Statistiques*, volume 47, pages 1029–1054, 2011.
- [6] Michał Balcerzak and Krzysztof Burnecki. Testing of fractional Brownian motion in a noisy environment. *Chaos, Solitons & Fractals*, 140:110097, 2020.
- [7] Albert Benassi, Stéphane Jaffard, and Daniel Roux. Elliptic Gaussian random processes. *Revista Matemática Iberoamericana*, 13(1):19–90, 1997.
- [8] Jan Beran. *Statistics for Long-memory Processes*. Routledge, 2017.
- [9] Hermine Biermé and Hans-Peter Scheffler. Fourier series approximation of linear fractional stable motion. *Journal of Fourier Analysis and Applications*, 14(2):180–202, 2008.
- [10] Tomasz Bojdecki, Luis G Gorostiza, and Anna Talarczyk. Sub-fractional Brownian motion and its relation to occupation times. *Statistics & Probability Letters*, 69(4):405–419, 2004.
- [11] Brahim Boufoussi, Marco Dozzi, and Raby Guerbaz. Path properties of a class of locally asymptotically self-similar processes. *Electronic Journal of Probability*, 13(29):898–921, 2008.
- [12] Grace Chan and Andrew T.A. Wood. Simulation of multifractional Brownian motion. In *COMPSTAT*, pages 233–238. Springer, 1998.
- [13] Jean-François Coeurjolly, Pierre-Olivier Amblard, and Sophie Achard. Wavelet analysis of the multivariate fractional Brownian motion. *ESAIM: Probability and Statistics*, 17:592–604, 2013.
- [14] Robert B Davies and D.S. Harte. Tests for Hurst effect. *Biometrika*, 74(1):95–101, 1987.
- [15] Yujia Ding, Qidi Peng, and Yimin Xiao. Linear multifractional stable sheets in the broad sense: existence and joint continuity of local times. *Bernoulli*, 29(1):785–814, 2023.
- [16] Vladimir Dobrić and Francisco M Ojeda. Fractional Brownian fields, duality, and martingales. *Lecture Notes-Monograph Series*, pages 77–95, 2006.

- [17] Roland Lvovich Dobrushin and Péter Major. Non-central limit theorems for non-linear functional of Gaussian fields. *Zeitschrift für Wahrscheinlichkeitstheorie und verwandte Gebiete*, 50:27–52, 1979.
- [18] Paul Doukhan, George Oppenheim, and Murad Taqqu. *Theory and Applications of Long-range Dependence*. Springer Science & Business Media, 2002.
- [19] Gregory S Elsaesser, Christian D Kummerow, Tristan S L’Ecuyer, Yukari N Takayabu, and Shoichi Shige. Observed self-similarity of precipitation regimes over the tropical oceans. *Journal of Climate*, 23(10):2686–2698, 2010.
- [20] Paul Embrechts. *Selfsimilar Processes*. Princeton University Press, 2009.
- [21] Patrick Flandrin. Wavelet analysis and synthesis of fractional Brownian motion. *IEEE Transactions on Information Theory*, 38(2):910–917, 1992.
- [22] I Haltas and ML Kavvas. Scale invariance and self-similarity in hydrologic processes in space and time. *Journal of Hydrologic Engineering*, 16(1):51–63, 2011.
- [23] Christian Houdré and José Villa. An example of infinite dimensional quasi-helix. *Contemporary Mathematics*, 336:195–202, 2003.
- [24] H-DJ Jeong, Don McNickle, and Krzysztof Pawlikowski. Fast self-similar teletraffic generation based on FGN and wavelets. In *IEEE International Conference on Networks. ICON’99 Proceedings (Cat. No. PR00243)*, pages 75–82. IEEE, 1999.
- [25] Hae-Duck J Jeong, K Pawlikowski, and DC McNickle. Generation of self-similar processes for simulation studies of telecommunication networks. *Mathematical and Computer Modelling*, 38(11-13):1249–1257, 2003.
- [26] Hae-Duck Joshua Jeong. *Modelling of Self-similar Teletraffic for Simulation*. PhD thesis, University of Canterbury, 2002.
- [27] Sixian Jin, Qidi Peng, and Henry Schellhorn. Estimation of the pointwise Hölder exponent of hidden multifractional Brownian motion using wavelet coefficients. *Statistical Inference for Stochastic Processes*, 21(1):113–140, 2018.
- [28] Andrei N Kolmogorov. Wienersche spiralen und einige andere interessante kurven in hilbertschen raum, cr (doklady). *Acad. Sci. URSS (NS)*, 26:115–118, 1940.
- [29] Nenghui Kuang and Huantian Xie. Asymptotic behavior of weighted cubic variation of sub-fractional Brownian motion. *Communications in Statistics-Simulation and Computation*, 46(1):215–229, 2017.
- [30] John Lamperti. Semi-stable stochastic processes. *Transactions of the American Mathematical Society*, 104(1):62–78, 1962.
- [31] Nick Laskin. Fractional Poisson process. *Communications in Nonlinear Science and Numerical Simulation*, 8(3-4):201–213, 2003.
- [32] Michel Ledoux and Michel Talagrand. *Probability in Banach Spaces: Isoperimetry and Processes*. Springer Science & Business Media, 2013.

- [33] Jacques Lévy-Véhel. Introduction to the multifractal analysis of images. *Fractal Image Encoding and Analysis*, 159:299–341, 1998.
- [34] Chungsheng Ma. The Schoenberg–Leévy kernel and relationships among fractional Brownian motion, bifractional Brownian motion, and others. *Theory of Probability & Its Applications*, 57(4):619–632, 2013.
- [35] Stephane G Mallat. A theory for multiresolution signal decomposition: the wavelet representation. *IEEE Transactions on Pattern Analysis and Machine Intelligence*, 11(7):674–693, 1989.
- [36] B Mandelbrot and J W van Ness. Fractional Brownian motions, fractional noises and applications. *SIAM Review*, 10(4):422–437, 1968.
- [37] Zbigniew Michna. Self-similar processes in collective risk theory. *International Journal of Stochastic Analysis*, 11(4):429–448, 1998.
- [38] Zbigniew Michna. On tail probabilities and first passage times for fractional Brownian motion. *Mathematical Methods of Operations Research*, 49:335–354, 1999.
- [39] Zbigniew Michna. *Ruin Probabilities and First Passage Times for Self-similar Processes*. PhD thesis, Department of Mathematical Statistics, Lund University, 2000.
- [40] Aneta Morozewicz and Darya Filatova. On the simulation of sub-fractional Brownian motion. In *2015 20th International Conference on Methods and Models in Automation and Robotics (MMAR)*, pages 400–405. IEEE, 2015.
- [41] Ilkka Norros, Esko Valkeila, and Jorma Virtamo. An elementary approach to a Girsanov formula and other analytical results on fractional Brownian motions. *Bernoulli*, 5(4):571–587, 1999.
- [42] Mathieu Rosenbaum. Estimation of the volatility persistence in a discretely observed diffusion model. *Stochastic Processes and their Applications*, 118(8):1434–1462, 2008.
- [43] Stefan Rostek and R Schöbel. A note on the use of fractional Brownian motion for financial modeling. *Economic Modelling*, 30:30–35, 2013.
- [44] G. Samorodnitsky and M. S. Taqqu. *Stable Non-Gaussian Random Processes*. Chapman & Hall/CRC, 1994.
- [45] Stilian Stoev and Murad S Taqqu. Simulation methods for linear fractional stable motion and FARIMA using the fast fourier transform. *Fractals*, 12(01):95–121, 2004.
- [46] Stilian A Stoev and Murad S Taqqu. How rich is the class of multifractional Brownian motions? *Stochastic Processes and their Applications*, 116(2):200–221, 2006.
- [47] Yue Sun, W Beck Andrews, Katsuyo Thornton, and Peter W Voorhees. Self-similarity and the dynamics of coarsening in materials. *Scientific Reports*, 8(1):17940, 2018.
- [48] Murad S Taqqu. Convergence of integrated processes of arbitrary hermite rank. *Zeitschrift für Wahrscheinlichkeitstheorie und verwandte Gebiete*, 50(1):53–83, 1979.
- [49] Murad S Taqqu. *Self-similar processes and related ultraviolet and infrared catastrophes*. Technical Report - School of Operations Research and Industrial Engineering, College of Engineering, Cornell University, 1979.

- [50] Brandon Whitcher. Simulating Gaussian stationary processes with unbounded spectra. *Journal of Computational and Graphical Statistics*, 10(1):112–134, 2001.
- [51] Andrew T A Wood and Grace Chan. Simulation of stationary Gaussian processes in  $[0, 1]^d$ . *Journal of Computational and Graphical Statistics*, 3(4):409–432, 1994.
- [52] Wei Biao Wu, George Michailidis, and Danlu Zhang. Simulating sample paths of linear fractional stable motion. *IEEE Transactions on Information Theory*, 50(6):1086–1096, 2004.